Inorg. Chem. **2005**, *44*, 4806–4817

Photoinduced Electron Transfer in Platinum(II) Terpyridinyl Acetylide Complexes Connected to a Porphyrin Unit

Cyrille Monnereau, Julio Gomez, Errol Blart, and Fabrice Odobel*

Laboratoire de Synthèse Organique, UMR 6513 CNRS, FR CNRS 2465, Faculté des Sciences et des Techniques de Nantes, BP 92208, 2 rue de la Houssinière, 44322 Nantes Cedex 03, France

Staffan Wallin, Anna Fallberg, and Leif Hammarström*

Department of Physical Chemistry, Uppsala University, Box 579, SE-751 23 Uppsala, Sweden

Received October 12, 2004

A series of six new dyads consisting of a zinc or magnesium porphyrin appended to a platinum terpyridine acetylide complex via a *para*-phenylene bisacetylene spacer are described. Different substituents on the 4′ position of the terpyridinyl ligand were explored (OC_7H_{15}, PO_3Et_2, and H). The ground-state electronic properties of the dyads are studied by electronic absorption spectroscopy and electrochemistry, and they indicate some electronic interactions between the porphyrin subunit and the platinum complex. The photophysical properties of these dyads were investigated by steady-state, time-resolved, and femtosecond transient absorption spectroscopy in N,N-dimethylformamide solution. Excitation of the porphyrin unit leads to a very rapid electron transfer (2–20 ps) to the nearby platinum complex followed by an ultrafast charge recombination, thus preventing any observation of the charge separated state. The variation in the rate of the photoinduced electron transfer in the series of dyads is consistent with Marcus theory. The results underscore the potential of the *para*-phenylene bisacetylene bridge to mediate a rapid electron transfer over a long donor–acceptor distance.

Introduction

The utilization of coordination compounds for the development of multicomponent photoactive systems is of great interest for applications in the area of solar energy conversion.[1−5] In this area, a great deal of attention has been particularly given to ruthenium,[5,6] osmium,[7] and rhenium polypyridine complexes[8] because of their outstanding photochemical properties due to their metal-to-ligand charge transfer (MLCT) excited state. More recently, several teams have shown the remarkable luminescent properties of acetylide platinum complexes that are potentially useful for the development of electroluminescent materials.[2,9,10,11] However, there are many fewer studies on the use of platinum(II) square-planar complexes for photoinduced electron or energy transfers. Arakawa and co-workers showed that platinum

* Author to whom correspondence should be addressed. E-mail: Fabrice.Odobel@chimie.univ-nantes.fr (F.O.).

(1) (a) Balzani, V.; Credi, A.; Scandola, F. *Math. Phys. Sci., Ser. C* **1994**, *448*, 1. (b) Balzani, V.; Bolletta, F.; Gandolfi, M. T.; Maestri, M. *Top. Curr. Chem.* **1978**, *75*, 1. (c) Schanze, K. S.; Walters, K. A. *Mol. Supramol. Photochem.* **1998**, *2*, 75. (d) Sauvage, J. P.; Collin, J. P.; Chambron, J. C.; Guillerez, S.; Coudret, C.; Balzani, V.; Barigelletti, F.; De Cola, L.; Flamigni, L. *Chem. Rev.* **1994**, *94*, 993. (e) Balzani, V.; Juris, A.; Venturi, M.; Campagna, S.; Serroni, S. *Chem. Rev.* **1996**, *96*, 759. (f) Scandola, F.; Chiorboli, C.; Indellli, M. T.; Eampo, M. A. *Electron Transfer in Chemistry*; Wiley-VCH: Weinheim, Germany, 2001; Vol. 3. (g) Meyer, T. J. *Acc. Chem. Res.* **1989**, *22*, 163. (h) Sun, L.; Hammarström, L.; Akermark, B.; Styring, S. *Chem. Soc. Rew.* **2001**, *30*, 36.

(2) Paw, W.; Cummings, S. D.; Mansour, M. A.; Connick, W. B.; Geiger, D. K.; Eisenberg, R. *Coord. Chem. Rev.* **1998**, *171*, 125.

(3) Hissler, M.; Connick, W. B.; Geiger, D. K.; McGarrah, J. E.; Lipa, D.; Lachicotte, R. J.; Eisenberg, R. *Inorg. Chem.* **2000**, *39*, 447.

(4) Kalyanasundaram, K. *Photochemistry of polypyridine and porphyrin complexes*; Academic Press: London, 1992.

(5) (a) Balzani, V.; Sabbatini, N.; Scandola, F. *Chem. Rev.* **1986**, *86*, 319. (b) Balzani, V.; Scandola, F. *Supramolecular Photochemistry*; Ellis Horwood: Chischester, U. K., 1991.

(6) (a) Dürr, H.; Bossmann, S. *Acc. Chem. Res.* **2001**, *34*, 905. (b) Flamigni, L.; Barigelletti, F.; Armaroli, N.; Collin, J.-P.; Dixon, I. M.; Sauvage, J.-P.; Williams, J. A. G. *Coord. Chem. Rev.* **1999**, *190−192*, 671.

(7) (a) De Cola, L.; Belser, P. *Coord. Chem. Rev.* **1998**, *177*, 301. (b) Belser, P.; Dux, R.; Baak, M.; De Cola, L.; Balzani, V. *Angew. Chem., Int. Ed. Engl.* **1995**, *34*, 595. (c) Belser, P.; Bernhard, S.; Blum, C.; Beyeler, A.; De Cola, L.; Balzani, V. *Coord. Chem. Rev.* **1999**, *190−192*, 155.

(8) (a) Beyeler, A.; Belser, P.; De Cola, L. *Angew. Chem., Int. Ed. Engl.* **1998**, *36*, 2779. (b) Ziessel, R.; Juris, A.; Venturi, M. *Inorg. Chem.* **1998**, *37*, 5061. (c) Schanze, K. S.; MacQueen, D. B.; Perkins, T. A.; Cabana, L. A. *Coord. Chem. Rev.* **1993**, *122*, 63.

10.1021/ic048573q CCC: $30.25
Published on Web 05/21/2005

diimine dithiolate complexes display promising properties for titanium dioxide sensitization, thus making these compounds suitable for dye-sensitized photovoltaic cells.[12] More recently, Eisenberg and co-workers reported several systems containing a platinum phenanthroline bis(arylacetylide) platinum complex connected to electron acceptors and donors that undergo efficient photoinduced charge separations.[13,14] Harriman and co-workers reported a fast intramolecular energy transfer from the second singlet excited-state of a zinc porphyrin to a ruthenium bipyridine fragment connected through a σ ethynyl platinum bisphosphine core.[15]

As an ongoing research program, we are interested in the development of electronically coupled multicomponent systems in order to perform light-induced functions such as a long-range electron transfer in a single step.[16,17] Platinum acetylide complexes with polypyridine ligands were appealing molecular building blocks for such a goal, because the carbon−platinum bond of the acetylide linkage may allow large electronic coupling with the neighboring unit. Furthermore, upon the photoinduced electron transfer, the reduced platinum complex could potentially be an active redox catalyst for water reduction.[18] More specifically, we were interested in merging the properties of the platinum complexes with those of a porphyrin chromophore. This latter fluorescent dye can serve as a light input element because it strongly absorbs in the visible spectrum,[4] and the terpyridine platinum acetylide complex could be the electron acceptor element of the photosystem. Another reason for choosing these molecular structures relies on the fact that, after the electron transfer from the porphyrin excited state, the negative charge is shifted further away from the oxidized porphyrin because the electron is localized in the terpyridine LUMO orbitals. As a result, the lifetime of the charge separated state may be significant.

In this work, we report on the preparation and the spectroscopic and electrochemical properties of a series of new dyads composed of a zinc or magnesium porphyrin linked to a platinum(II) acetylide terpyridine complex (cf. Scheme 1). By changing the substituent of the terpyridine ligand and the metal complexed inside the porphyrin of these dyads, it was possible to tune the redox potentials and the excited-state properties of each module. As a result, the quenching rate of the porphyrin singlet excited state in the dyads can be varied.

Scheme 1 . Structures of the Molecules Studied in This Work

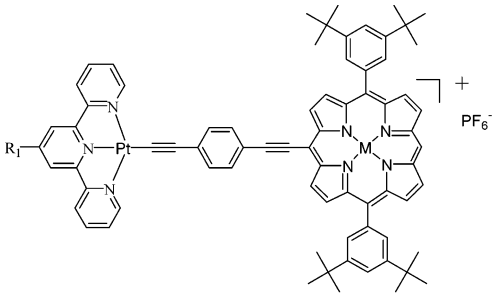

15 : R_1= PO_3Et_2, M = Zn^{II} **18** : R_1= PO_3Et_2, M = Mg^{II}

16 : R_1= H, M = Zn^{II} **19** : R_1= H, M = Mg^{II}

17: R_1= OC_7H_{15} , M = Zn^{II} **20**: R_1= OC_7H_{15} , M = Mg^{II}

Experimental Section

General Methods. ^{1}H NMR spectra were recorded on a Bruker ARX 400 MHz Bruker spectrometer. Chemical shifts for ^{1}H NMR spectra are referenced relative to the residual protium in the deuterated solvent ($CDCl_3$, δ = 7.26 ppm). Mass spectra were recorded on an EI−MS HP 5989A spectrometer or a JMS-700 (JEOL Ltd, Akishima, Tokyo, Japan) double-focusing mass spectrometer of reversed geometry equipped with an electrospray ionization source. Thin-layer chromatography was performed on aluminum sheets precoated with Merck 5735 Kieselgel 60F_{254}. Column chromatography was carried out either with Merck 5735 Kieselgel 60F (0.040−0.063 mm mesh) or with SDS neutral alumina (0.05−0.2 mm mesh). Air-sensitive reactions were carried out under argon in dry solvents and glassware. Chemicals were purchased from Aldrich and used as received. Compounds tetrakis-(trisphenyl)phosphine palladium,[19] [Pt(COD)Cl_2],[20] terpyridinePtCl complex **5**[21], 2,6-di-2-pyridyl-4(1H)-pyridone,[22] 2,2′:6′,0.2″-terpyridine, and 4′-[((trifluoromethyl)sulfonyl)oxy]-2,2′:6′.2″-terpyridine[22] were prepared according to literature methods.

UV−visible absorption spectra were recorded on a UV-2401PC Shimadzu spectrophotometer. Fourier transform infrared spectra were recorded in pressed KBr pellets on a Bruker Vector 22 spectrometer.

The electrochemical measurements were performed with a potentiostat−galvanostat MacLab model ML160 controlled by resident software (Echem version 1.5.2 for Windows) using a conventional single-compartment three-electrode cell. The working electrode was a Pt wire 10 mm long, the auxiliary was a Pt wire, and the reference electrode was the saturated potassium chloride calomel electrode (SCE). The supported electrolyte was 0.1 N Bu_4NPF_6 in N,N-dimethylformamide (DMF), and the solutions were purged with argon before the measurements. All potentials are

(9) (a) Chan, S.-C.; Chan, M. C. W.; Wang, Y.; Che, C.-M.; Cheung, K.-K.; Zhu, N. *Chem.—Eur. J.* **2001**, *7*, 4180. (b) Whittle, C. E.; Weinstein, J. A.; George, M. W.; Schanze, K. S. *Inorg. Chem.* **2001**, *40*, 4053. (c) Cummings, S. D.; Eisenberg, R. *Inorg. Chem.* **1995**, *34*, 2007. (d) Michalec, J. F.; Bejune, S. A.; McMillin, D. R. *Inorg. Chem.* **2000**, *39*, 2708. (e) Yam, V. W.-W. *Acc. Chem. Res.* **2002**, *35*, 555.
(10) Yam, V. W.-W.; Tang, R. P.-L.; Wong, K. M.-C.; Cheung, K.-K. *Organometallics* **2001**, *20*, 4476.
(11) Yang, Q.-Z.; Wu, L.-Z.; Wu, Z.-X.; Zhang, L.-P.; Tung, C.-H. *Inorg. Chem.* **2002**, *41*, 5653.
(12) (a) Islam, A.; Sugihara, H.; Hara, K.; Pratap Singh, L.; Katoh, R.; Yanagida, M.; Takahashi, Y.; Murata, S.; Arakawa, H. *New J. Chem.* **2000**, *24*, 343. (b) Islam, A.; Sugihara, H.; Hara, K.; Singh, L. P.; Katoh, R.; Yanagida, M.; Takahashi, Y.; Murata, S.; Arakawa, H.; Fujihashi, G. *Inorg. Chem.* **2001**, *40*, 5371.
(13) McGarrah, J. E.; Kim, Y.-J.; Hissler, M.; Eisenberg, R. *Inorg. Chem.* **2001**, *40*, 4510.
(14) McGarrah, J. E.; Eisenberg, R. *Inorg. Chem.* **2003**, *42*, 4355.
(15) Harriman, A.; Hissler, M.; Trompette, O.; Ziessel, R. *J. Am. Chem. Soc.* **1999**, *121*, 2516.
(16) Odobel, F.; Suresh, S.; Blart, E.; Nicolas, Y.; Quintard, J.-P.; Janvier, P.; Le Questel, J.-Y.; Illien, B.; Rondeau, D.; Richomme, P.; Haupl, T.; Wallin, S.; Hammarström, L. *Chem.—Eur. J.* **2002**, *8*, 3027.
(17) Blart, E.; Suzenet, F.; Quintard, J.-P.; Odobel, F. *J. Porphyrins Phthalocyanines* **2003**, *7*, 207.
(18) Zhang, D.; Wu, L.-Z.; Li, Z.; Han, X.; Yang, Q.-Z.; Zhang, L.-P.; Tung, C.-H. *J. Am. Chem. Soc.* **2004**, *126*, 3440.
(19) Schlosser, M. *Organometallics in Synthesis: A Manual*; Wiley and Sons: New York, 1994.
(20) Peters, T. B.; Bohling, J. C.; Arif, A. M.; Gladysz, J. A. *Organometallics* **1999**, *18*, 3261.
(21) Hobert, S. E.; Carney, J. T.; Cummings, S. D. *Inorg. Chim. Acta* **2001**, *318*, 89.
(22) Potts, K. T.; Konwar, D. *J. Org. Chem.* **1991**, *56*, 4815.

quoted relative to SCE. In all of the experiments, the scan rate was 100 mV/s for cyclic voltammetry and 15 Hz for pulse voltammetry.

Fluorescence spectra were recorded on a SPEX Fluorolog II Systems fluorimeter and were corrected for the wavelength-dependent response of the detector system. Fluorescence lifetimes were determined using a time-correlated single-photon counting setup. The samples were excited at 400 nm with 200 kHz, 150 fs laser pulses by frequency-doubling the output from an amplified Ti:sapphire laser system. The emission was detected at a right angle using magic angle polarizers and 470 nm cutoff filters to remove scattered excitation light. The full width at half maximum (fwhm) of the response function measured from a scattering sample was about 70 ps.

Femtosecond transient absorption measurements were made using an amplified 1 kHz Ti:sapphire laser system. An optical parametric amplifier (TOPAS) was used to produce 630 nm, 120 fs excitation pulses. The pump passed a chopper in which every other pulse was blocked before it was focused in the sample cell (1 mm quartz cuvette). The sample cell was mounted on a holder that moved up and down with a frequency of about 1 Hz. The probe beam was led through a delay line and focused on a CaF_2 plate where a white light continuum (WL) was generated. A beam splitter was used to produce a WL reference beam. The probe and reference were focused through the slit of a monochromator and detected by two 512 pixel diode arrays. The transient absorption signal was calculated for each pair of shots (pump−probe vs probe only) and then averaged. Transient absorption spectra are the average of 10 scans with 1000 shots at each time step. The absorbance of the sample was about 0.3 at the excitation wavelength. The response function measured as the fwhm of the signal from pure solvent is 150−200 fs. The transient spectra were corrected for the spectral chirp (200−300 fs over the detected spectral window) by visually determining the zero time location in the 3D data file.

4′-Diethylphosphonate-2,2′:6′,2″-terpyridine (1). Diethyl phosphite (2 mL, 15.7 mmol), Et_3N (1.46 mL, 10.5 mmol), PPh_3 (6.9 g, 26.3 mmol), and $Pd(Ph_3)_4$ (0.67 g, 0.6 mmol) were added to a suspension of 4′-triflate-2,2′:6′,2″-terpyridine (2 g, 5.3 mmol) in distilled toluene (80 mL). The reaction mixture was set under argon and heated to reflux. After 12 h, the mixture was evaporated to dryness. The resulting crude reaction mixture was purified by column chromatography on silica (eluted with a gradient of AcOEt in petroleum ether, from 10 to 70%). A white solid was isolated, **1** (1.2 g, yield 92%). ^{1}H NMR (200 MHz, $CDCl_3$) δ: 8.85 (d, 2H, ^3J_p = 14 Hz), 8.72 (m, 2H), 8.60 (dt, 2H, ^4J = 1.1 Hz, ^3J = 7.9 Hz), 7.87 (ddd, 2H, ^4J = 1.8 Hz, ^3J = 7.6 Hz, ^3J = 7.9 Hz), 7.36 (ddd, 2H, ^4J = 1.1 Hz, ^3J = 4.9 Hz, ^3J = 7.6 Hz), 4.27 (m, 4H), 1.35 (t, 6H, ^3J = 7.2 Hz). MS−EI (*m*/*z*) Calcd for $C_{19}H_{20}N_3O_3P$ = 369.1. Found = 369.1 $(M)^+$.

4′-Heptoxy-2,2′:6′,2″-terpyridine (3). 1-Bromoheptane (1.3 mL) and KOH (1.5 g) were added to a suspension of dipyridilpyridone (0.300 g, 1.2 mmol) in acetone (21 mL) and DMF (8 mL). This stirred suspension was heated to reflux for 5 h. The mixture was evaporated to dryness. A total of 100 mL of water was added, and the solution was extracted with CH_2Cl_2 (3 × 100 mL). The combined organic layers were dried on $MgSO_4$ and filtered. The resulting pale yellow solution was evaporated to dryness, and the crude product was purified by column chromatography on neutral alumina (petroleum ether/AcOEt, 90:10). A white solid was isolated, **3** (0.342 g, yield 82%). ^{1}H NMR (200 MHz, $CDCl_3$) δ: 8.10 (d, 2H, ^3J = 4.2 Hz), 8.04 (d, 2H, ^3J = 8.0 Hz), 7.43 (d, 2H, ^3J = 7.9 Hz), 7.27 (dd, ^3J = 7.1 Hz, ^3J = 7.1 Hz), 6.74 (dd, 2H, ^3J = 7.1 Hz, ^3J = 5.4 Hz), 3.64 (t, 2H, ^3J = 6.2 Hz), 0.5−1.6 (m, 11H). MS−EI (*m*/*z*) Calcd for $C_{22}H_{25}N_3O$ = 347.2. Found = 347.2 $(M)^+$.

Pt Complex with 4′-Diethylphosphonate-2,2′:6′,2″-terpyridine (4). Terpyridine diethylphosphonate, **1** (0.098 g, 0.266 mmol), was added to a suspension of $[Pt(COD)Cl_2]$ (0.100 g, 0.266 mmol) in water (20 mL). The stirred suspension was heated to 60 °C for 1 h, and the resulting orange solution was filtered over Celite. To the filtrate was added an aqueous solution of $NaBF_4$ (0.2 g of $NaBF_4$ in 5 mL of water). The solution was cooled in an ice bath, and the orange precipitate was filtered and repeatedly washed with water, then with diethyl ether. Upon drying under a vacuum, an orange solid was isolated, **4** (0.176 g, yield 93%). ^{1}H NMR (400 MHz, d_6-DMSO) δ: 8.98 (d, 2H, ^3J = 5.6 Hz), 8.96 (d, 2H, ^3J = 8 Hz), 8.83 (d, 2H, ^3J = 13.2 Hz), 8.53 (dd, 2H, ^3J = 8 Hz, ^3J = 7.1 Hz), 8.00 (dd, 2H, ^3J = 7.1 Hz, ^3J = 5.6 Hz), 4.25 (m, 4H), 1.33 (m, 6H). IR (KBr disk, ν/cm^{-1}): 3048 (m), 1606 (s), 1413 (s), 1143 (s), 1034 (m), 785 (s), 596 (s). MS−FAB (*m*/*z*) Calcd for $C_{19}H_{20}ClN_3O_3PPt$ = 599.1. Found = 599.9 $(M)^+$.

Pt Complex with 4′-Heptoxy-2,2′:6′,2″-terpyridine (6). To a suspension of $[Pt(COD)Cl_2]$ (0.162 g, 0.432 mmol) in water (30 mL) was added 0.150 g (0.432 mmol) of **3**, and the suspension was heated to 60 °C for 1 h. The resulting yellow solution was filtered over Celite. To the filtrate was added a solution of 0.2 g of $NaBF_4$ in water (5 mL), giving rise to a red-orange precipitate. The suspension was cooled in an ice bath. The solid was filtered and repeatedly washed with water and diethyl ether. Upon drying under a vacuum, a red-orange solid was isolated, **6** (0.265 g, yield 92%). ^{1}H NMR (400 MHz, d_6-DMSO) δ: 8.86 (d, 2H, ^3J = 5.2 Hz), 8.64 (d, 2H, ^3J = 8.0 Hz), 8.50 (dd, 2H, ^3J = 8.0 Hz, ^3J = 7.2 Hz), 8.27 (s, 2H), 7.92 (dd, 2H, ^3J = 7.2 Hz, ^3J = 5.2 Hz), 4.36 (m, 2H), 1.86 (m, 2H), 0.80−1.50 (m, 11H). IR (KBr disk, ν/cm^{-1}): 2926 (m), 1617 (s), 1608 (s), 1480 (s), 1434 (s), 1225 (s), 1084 (m), 784 (s). MS−FAB (*m*/*z*) Calcd for $C_{22}H_{25}ClN_3OPPt$ = 577.1. Found = 578.0 $(M)^+$.

General Procedure for the Preparation of Platinum Terpyridyl Acetylide Complexes (12−14). 1-Ethynyl-4-triisopropylsilylethynylbenzene, **7** (0.050 g, 0.1775 mmol); CuI (5 mg); and ^{i}Pr$_2$NH (1 mL) were added to a suspension of $[(R_1\text{-trpy})PtCl](BF_4)$ (0.16 mmol) in distilled CH_2Cl_2 (20 mL) under argon. The mixture was stirred overnight at room temperature and resulted in a reddish colored suspension. The solid was filtered and washed with CH_2Cl_2, and then tetrahydrofuran (THF). Upon drying under a vacuum, the awaited product was isolated.

[Pt(trpyPO$_3$Et$_2$)(C≡CC$_6$H$_4$C≡CTIPS)]BF$_4$ (12). Complex **12** was isolated as a deep red solid, yield 51%. ^{1}H NMR (400 MHz, d_6-DMSO) δ: 9.22 (d, 2H, ^3J = 5.3 Hz), 8.95 (d, 2H, ^3J = 7.9 Hz), 8.87 (d, 2H, ^3J = 13.2 Hz), 8.53 (dd, 2H, ^3J = 7.9 Hz, ^3J = 6.5 Hz), 7.99 (dd, 2H, ^3J = 6.5 Hz), 7.53 (d, 2H, ^3J = 8 Hz), 7.44 (d, 2H, ^3J = 8 Hz), 4.24 (m, 4H), 1.35 (t, 6H, ^3J = 6.6 Hz), 1.13 (s, 21H). IR (KBr disk, ν/cm^{-1}): 2942 (m), 2864 (s), 2150 (s), 2118 (s), 1605 (s), 1409 (s), 1098 (m), 781 (s), 474 (s). MS−FAB (*m*/*z*) Calcd for $C_{38}H_{45}N_3O_3PPtSi$ = 845.2. Found = 845.9 $(M)^+$.

[Pt(trpy)(C≡CC$_6$H$_4$C≡CTIPS)]BF$_4$ (13). Complex **13** was isolated as a garnet solid, yield 45%. ^{1}H NMR (400 MHz, d_6-DMSO) δ: 9.02 (d, 2H, ^3J = 6.2 Hz), 8.6−8.5 (m, 5H), 8.46 (dd, 2H, ^3J = 8.0 Hz, ^3J = 7.1 Hz), 7.88 (dd, 2H, ^3J = 6.2 Hz, ^3J = 7.1 Hz), 7.44 (2d, 4H, ^3J = 8.4 Hz), 1.13 (s, 21H). IR (KBr disk, ν/cm^{-1}): 2944 (m), 2865 (s), 2152 (s), 2120 (s), 1711(s), 1604 (s), 1455 (s), 1109 (m), 839 (m), 771 (s), 559 (s). MS−FAB (*m*/*z*) Calcd for $C_{34}H_{36}N_3PtSi$ = 709.2. Found = 709.3 $(M)^+$.

[Pt(C$_7$H$_{15}$O-trpy)(C≡CC$_6$H$_4$C≡CTIPS)]BF$_4$ (14). Complex **14** was isolated as a red solid, yield 92%.^{1}H NMR (400 MHz, d_6-acetone) δ: 9.32 (d, 2H, ^3J = 5.5 Hz), 8.68 (d, 2H, ^3J = 8 Hz), 8.53 (dd, 2H, ^3J = 8.0 Hz, ^3J = 7.0 Hz), 8.28 (s, 2H), 7.96 (dd, 2H, ^3J = 7 Hz, ^3J = 5.5 Hz), 7.47 (d, 4H,^3J = 8 Hz), 4.47 (t, 2H,

^3J = 8 Hz), 1.36 (s, 36H), 1.3−1.18 (m, 12H), 0.89 (3H, t). IR (KBr disk, ν/cm^{-1}): 2960 (m), 2865 (s), 2151 (s), 2118 (s), 1616 (s), 1608 (s),1463 (s), 1099 (m), 801 (m), 473 (s). MS−FAB (*m*/*z*) Calcd for $C_{41}H_{50}N_3OPtSi$ = 823.3. Found = 823.3 $(M)^+$.

5-((4′-Trisisopropylsilylethynylphenyl)ethynyl)-10,15-bis-(3′,5′-di-*tert*-butylphenyl)-porphyrin (8). 1-Ethynyl-4-triisopropylsilyl-ethynylbenzene, **7** (0.250 g, 0.887 mmol), and distilled Et_3N (7 mL) were added to a solution of 10-bromo-5,15-bis-(3,5-di-*tert*-butyl-phenyl)-porphyrin (0.390 g, 0.506 mol) in distilled toluene (33 mL). This solution was degassed by 15 min of N_2 bubbling under sonication. $AsPh_3$ (38 mg, 0.124 mmol) and $Pd_2(dba)_3$−$CHCl_3$ (39 mg, 0.038 mmol) were then added. The dark red solution was once again degassed. The stirred reaction mixture was then heated at 60 °C for 20 h. The solvents were removed by rotary evaporation, and the crude product was purified by flash column chromatography on silica gel, eluted with a mixture of CH_2Cl_2/petroleum ether (20:80), leading to a brown solid, **8** (408 mg, yield 81%). ^{1}H NMR (200 MHz, $CDCl_3$) δ: 10.17 (s, 1H), 9.82 (d, 2H, ^3J = 4.5 Hz), 9.29 (d, 2H, ^3J = 4.5 Hz), 9.03 (d, 2H, ^3J = 5.6 Hz), 9.00 (d, 2H, ^3J = 5.6 Hz), 8.12 (s, 4H), 7.98 (d, 2H, ^3J = 8.1 Hz), 7.84 (s, 2H), 7.68 (d, 2H, ^3J = 8.1 Hz), 1.57 (s, 36H), 1.20 (s, 21H), −2.46 (s, 2H). IR (KBr disk, ν/cm^{-1}): 2963 (m), 2864 (s), 2150 (s), 1462 (s), 1261 (s), 1097 (m), 799 (m). MS−FAB (*m*/*z*) Calcd for $C_{67}H_{78}N_4Si$ = 966.6. Found = 967.8 $(M + H)^+$.

5-((4′-Ethynylphenyl)ethynyl)-10,15-bis-(3′,5′-di-*tert*-butylphenyl)-porphyrin (9). Bu_4NF (1M in THF, 0.57 mL) was added to a solution of the porphyrin **8** (0.140 g, 0.142 mmol) in distilled THF (150 mL). The reddish solution was stirred at room temperature under argon for 1 h and turned to dark green. A total of 100 mL of brine was added to the reaction mixture, and the solution was extracted with CH_2Cl_2 (3 × 100 mL). The combined organic layers were dried on $MgSO_4$ and filtered, and the solvent was removed by rotary evaporation. The crude product was purified by flash column chromatography on silica gel (eluted with a mixture of CH_2Cl_2/petroleum ether/Et_3N, 19:80:1). A blue-green solid was isolated, **9** (110 mg, yield 93%). ^{1}H NMR (400 MHz, $CDCl_3$) δ: 10.19 (s, 1H), 9.85 (d, 2H, ^3J = 4.3 Hz), 9.36 (d, 2H, ^3J = 4.3 Hz), 9.08 (d, 2H, ^3J = 4.3 Hz), 9.01 (d, 2H, ^3J = 4.3 Hz), 8.12 (s, 4H), 7.98 (d, 2H, ^3J = 9.8 Hz), 7.83 (s, 2H), 7.70 (d, 2H, ^3J = 9.8 Hz), 3.22 (s, 1H), 1.55 (s, 36H), −2.91 (s, 2H). IR (KBr disk, ν/cm^{-1}): 2961 (m), 2183 (s), 2110 (s), 1465 (m), 1368 (s), 1075 (m), 765 (m). MS−FAB (*m*/*z*) Calcd for $C_{58}H_{58}N_4$ = 810.5. Found = 811.7 $(M + H)^+$.

[5-((4′-Ethynylphenyl)ethynyl)-10,15-bis-(3′,5′-di-*tert*-butylphenyl)-porphyrinato] Zinc(II) (10). A solution of $Zn(OAc)_2 \cdot 2H_2O$ (0.454 g, 2.07 mmol) in 25 mL of MeOH was added to a solution of **9** (0.100 g, 0.1034 mmol) in CH_2Cl_2 (50 mL). The reddish reaction mixture was then stirred at room temperature for 1 h, and the solvents were rotary evaporated. The green solid was solubilized in dichloromethane, and the solution was washed with 100 mL of water. The organic layer was dried with $MgSO_4$ and filtered, and the solvent was removed by rotary evaporation. A green solid was isolated, **10** (0.105 mg, yield 99%). ^{1}H NMR (200 MHz, $CDCl_3$) δ: 10.15 (s, 1H), 9.82 (d, 2H, ^3J = 4.3 Hz), 9.30 (d, 2H, ^3J = 3.6 Hz), 9.09 (d, 2H, ^3J = 4.0 Hz), 9.03 (d, 2H, ^3J = 4.0 Hz), 8.11 (s, 4H), 7.95 (2H, d, ^3J = 7.7 Hz), 7.84 (s, 2H), 7.66 (d, 2H, ^3J = 7.7 Hz), 1.58 (s, 36H). IR (KBr disk, ν/cm^{-1}): 2961 (m), 2868 (s), 2186 (s), 2107 (s), 1592 (s), 1463 (m), 1384 (s), 1363 (s), 1259 (s), 1060 (m), 793 (s). MS−FAB (*m*/*z*) Calcd for $C_{58}H_{56}N_4Zn$ = 872.4. Found = 874.5 $(M)^+$.

General Procedure for the Preparation of Dyads Containing Zinc Porphyrin (15−17). To a solution of porphyrin **10** (38.3 mg, 0.0437 mmol) in distilled CH_2Cl_2 (40 mL) were added the terpyridine platinum complex [(R_1-trpy)Pt Cl](PF_6) (0.035 mmol), CuI (4 mg), and ^{i}Pr$_2$NH (1 mL). The suspension was then stirred overnight at room temperature. The resulting mixture was filtered on Celite, and the Celite was washed with CH_2Cl_2. The filtrate was evaporated to dryness. The residue was solubilized in CH_2Cl_2 (4 mL), precipitated with petroleum ether (20 mL), and filtered. The green solid was then washed with a mixture of CH_2Cl_2/petroleum ether (1:5). Finally, the complex was solubilized in THF, precipitated with an aqueous solution of KPF_6, and filtered, and the precipitate was washed with water.

[(Et_2O_3P-trpy)Pt(C≡CC_6H_4C≡C−ZnP)]PF_6 (15). Yield 61%. R_f = 0.21 on neutral alumina eluted with CH_2Cl_2/CH_3OH (98:2). ^{1}H NMR (400 MHz, d_6-DMSO) δ: 10.29 (s, 1H), 9.85 (d, 2H, ^3J = 5.2 Hz), 9.45 (d, 2H, ^3J = 5.2 Hz), 9.32 (d, 2H, ^3J = 4.7 Hz), 8.80−9.05 (m, 8H), 8.56 (m, 4H), 8.15 (2H, d, ^3J = 7.8 Hz), 8.07 (s, 4H), 7.88 (s, 2H), 7.8 (d, 2H, ^3J = 7.8 Hz), 4.53 (m, 4H), 1.54 (s, 36H), 0.95 (m, 6H). IR (KBr disk, ν/cm^{-1}): 2961 (m), 2182 (s), 2115 (s), 1591 (s), 1061 (m), 792 (m). MS−FAB (*m*/*z*) Calcd for $C_{77}H_{75}N_7O_3PPtZn$ = 1435.5. Found = 1437.9 $(M)^+$.

[(trpy)Pt(C≡CC_6H_4C≡C−ZnP)]PF_6 (16). Yield 72%. R_f = 0.36 on neutral alumina eluted with CH_2Cl_2/CH_3OH (98:2). ^{1}H NMR (400 MHz, d_6-DMSO) δ: 10.30 (s, 1H), 9.83 (d, 2H, ^3J = 5.5 Hz), 9.45 (d, 2H, ^3J = 5.5 Hz), 9.30 (d, 2H, ^3J = 3.2 Hz), 8.95 (d, 2H, ^3J = 5.0 Hz), 8.89 (d, 2H, ^3J = 5.0 Hz), 8.5−8.75 (m, 5H), 8.14 (d, 2H, ^3J = 7.8 Hz), 8.07 (s, 4H), 8.01 (m, 2H), 7.88 (s, 2H), 7.78 (d, 2H, ^3J = 8 Hz), 1.53 (s, 36H). IR (KBr disk, ν/cm^{-1}): 2960 (m), 2868 (s), 2184 (s), 2113 (s), 1591 (s), 1475 (s), 1453 (s), 1247 (s), 1208 (s), 844 (m). MS−FAB (*m*/*z*) Calcd for $C_{73}H_{66}N_7PtZn$ = 1299.4. Found = 1300.0 $(M)^+$.

[(C_7H_{15}Otrpy)Pt(C≡CC_6H_4C≡C−ZnP)]PF_6 (17). Yield 45%. R_f = 0.20 on neutral alumina eluted with CH_2Cl_2/CH_3OH (98:2). ^{1}H NMR (400 MHz, d_6-DMSO) δ:10.23 (s, 1H), 9.82 (d, 2H, ^3J = 6 Hz), 9.43 (d, 2H, ^3J = 6 Hz), 9.15 (m, 2H), 8.94 (d, 2H, ^3J = 4.8 Hz), 8.88 (d, 2H, ^3J = 4.8 Hz), 8.64 (m, 2H), 8.50 (m, 2H), 8.23 (m, 2H), 8.11 (d, 2H, ^3J = 8.1 Hz), 8.07 (s, 4H), 7.91 (m, 2H), 7.88 (s, 2H), 7.73 (d, 2H, ^3J = 8.1 Hz), 4.27 (m, 2H), 1.56 (s, 36H), 0.8−1.4 (m, 13H). IR (KBr disk, ν/cm^{-1}): 2960 (m), 2870 (m), 2184 (s), 2113 (s), 1607 (s), 1209 (s), 1084 (m), 793 (s). MS−FAB (*m*/*z*) Calcd for $C_{80}H_{80}N_7OPtZn$ = 1413.5. Found = 1414.0 $(M)^+$.

[5-((4′-Ethynylphenyl)ethynyl)-10,15-bis-(3′,5′-di-*tert*-butylphenyl)-porphyrinato]magnesium(II) (11). To a solution of the porphyrin **9** (110 mg, 0.137 mmol) in distilled CH_2Cl_2 (9 mL) were added distilled ^{i}Pr$_2$NH (0.5 mL) and magnesium iodide (380 mg, 1.37 mmol). The green solution was stirred at room temperature under argon for 30 min. A total of 20 mL of water was then added, and the solution was extracted with CH_2Cl_2 (3 × 20 mL). The combined organic layers were dried on $MgSO_4$ and filtered, and the solvent was removed by rotary evaporation. The crude product was purified by column chromatography on alumina gel (eluted with a mixture of CH_3CN/Et_3N, 99:1). A bright green product was isolated, **11** (88 mg, yield 78%). ^{1}H NMR (400 MHz, $CDCl_3$) δ: 10.12 (s, 1H), 9.86 (d, 2H, ^3J = 4.3 Hz), 9.28 (d, 2H, ^3J = 4.3 Hz), 9.04 (d, 2H, ^3J = 4.3 Hz), 8.99 (d, 2H, ^3J = 4.3 Hz), 8.11 (s, 4H), 7.98 (d, 2H, ^3J = 8.4 Hz), 7.81 (s, 2H), 7.72 (d, 2H, ^3J = 8.4 Hz), 3.22 (s, 1H), 1.57 (s, 36H), −2.90 (s, 2H). IR (KBr disk, ν/cm^{-1}): 2960 (m), 2184 (s), 2108 (s), 1590 (s), 1460 (m), 1375 (s), 1260 (s), 1060 (m), 792 (s). MS−ES (*m*/*z*) Calcd for $C_{59}H_{60}MgON_4$ = 864.46. Found = 864.46 $(M + CH_3OH)^+$.

General Procedure for the Preparation of the Dyads Containing a Magnesium Porphyrin (18−20). To a solution of the porphyrin **11** (25 mg, 0.030 mmol) were added ^{i}Pr$_2$NH (0.5 mL), CuI (1 mg), and the platinum terpyridine complex (0.025 mmol)

Scheme 2 . General Route for the Preparation of the Platinum Complexes Studied in This Work

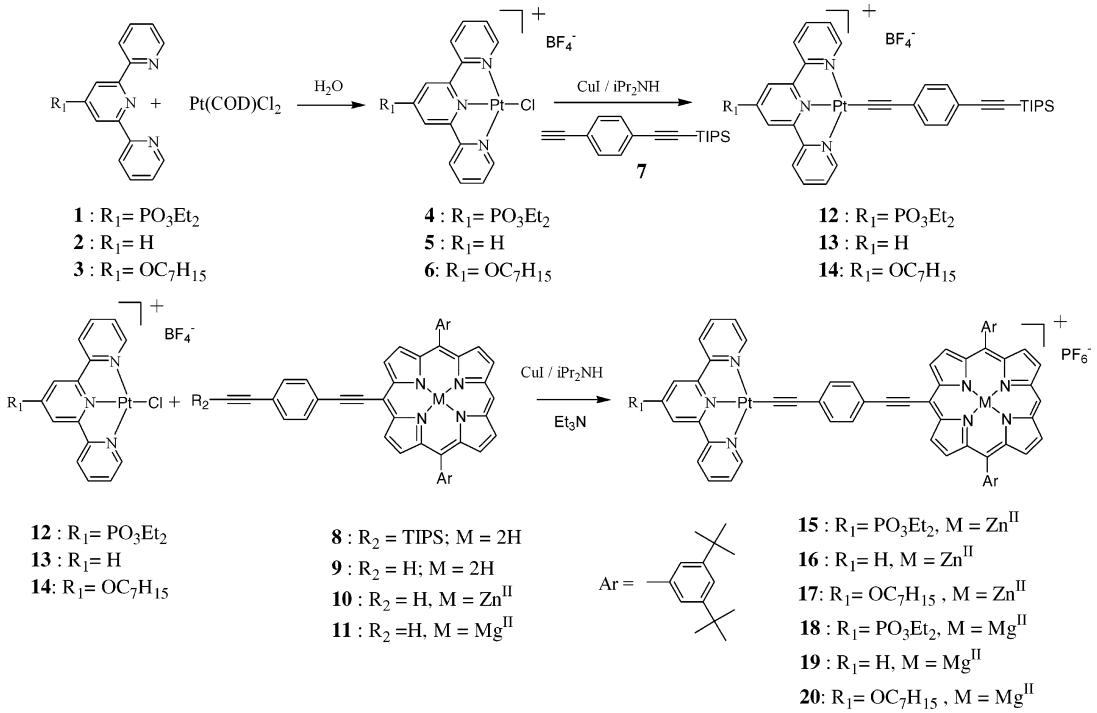

1 : R_1= PO_3Et_2
2 : R_1= H
3 : R_1= OC_7H_{15}

4 : R_1= PO_3Et_2
5 : R_1= H
6: R_1= OC_7H_{15}

12 : R_1= PO_3Et_2
13 : R_1= H
14: R_1= OC_7H_{15}

12 : R_1= PO_3Et_2
13 : R_1= H
14: R_1= OC_7H_{15}

8 : R_2 = TIPS; M = 2H
9 : R_2 = H; M = 2H
10 : R_2 = H, M = Zn^{II}
11 : R_2 =H, M = Mg^{II}

15 : R_1= PO_3Et_2, M = Zn^{II}
16 : R_1= H, M = Zn^{II}
17: R_1= OC_7H_{15} , M = Zn^{II}
18 : R_1= PO_3Et_2, M = Mg^{II}
19 : R_1= H, M = Mg^{II}
20: R_1= OC_7H_{15} , M = Mg^{II}

in distilled CH_2Cl_2 (25 mL). The mixture was stirred overnight at room temperature under argon. The mixture turned to very dark green. For **18**, a precipitate formed during the reaction, and it was directly filtered. This precipitate was then washed with petroleum ether (30 mL) and then with CH_2Cl_2 (60 mL).

The procedure was slightly different for **19** and **20,** where no precipitate appeared. A total of 30 mL of water was added to the reaction mixture, and the solution was extracted with CH_2Cl_2 (3 × 20 mL). The combined organic layers were dried on $MgSO_4$ and filtered, and the solvent was removed by rotary evaporation. The dark green residue was solubilized in THF, precipitated with an aqueous solution of KPF_6, and filtered. Finally, the filtrate was washed with water and then with diethyl ether.

[(Et_2O_3P-trpy)Pt(C≡CC_6H_4C≡C−MgP)]PF_6 (18). Yield 60%. R_f = 0.21 on neutral alumina eluted with CH_2Cl_2/CH_3OH (98:2). ^{1}H NMR (400 MHz, d_6-DMSO) δ: 10.28 (s, 1H), 9.82 (d, 2H, ^3J = 5.5 Hz), 9.40 (d, 2H, ^3J = 5.5 Hz), 9.35 (d, 2H, ^3J = 5.5 Hz), 8.80−9.05 (m, 8H), 8.58 (t, 2H, ^3J = 7.8 Hz), 8.54 (t, 2H, ^3J = 7.8 Hz), 8.14 (d, 2H, ^3J = 8 Hz), 8.10 (s, 4H), 7.88 (s, 2H), 7.78 (d, 2H, ^3J = 8 Hz), 4.53 (m, 4H), 1.54 (s, 36H), 0.95 (m, 6H). IR (KBr disk, ν/cm^{-1}): 2960 (m), 2182 (s), 2117 (s), 1590 (s), 1045 (m), 791 (m). MS−FAB (*m*/*z*) Calcd for $C_{77}H_{75}MgN_7O_3PPt$ = 1396.5. Found = 1396.3 $(M)^+$.

[(trpy)Pt(C≡CC_6H_4C≡C−MgP)]PF_6 (19). Yield 83%. R_f = 0.36 on neutral alumina eluted with CH_2Cl_2/CH_3OH (98:2). ^{1}H NMR (400 MHz, d_6-DMSO) δ: 10.27 (s, 1H), 9.81 (d, 2H, ^3J = 5.5 Hz), 9.39 (d, 2H, ^3J = 5.5 Hz), 9.26 (m, 2H), 8.91 (d, 2H, ^3J = 5.2 Hz), 8.84 (d, 2H, ^3J = 5.2 Hz), 8.65 (m, 5H), 8.54 (m, 2H), 8.13 (d, 4H, ^3J = 7.8 Hz), 8.08 (s, 4H), 8.00 (m, 2H), 7.87 (s, 2H), 7.78 (d, 2H, ^3J = 7.8 Hz), 1.56 (s, 36H). IR (KBr disk, ν/cm^{-1}): 2960 (m), 2180 (s), 2114 (s), 1590 (s), 1210 (s), 838 (m). MS−FAB (*m*/*z*) Calcd for $C_{73}H_{66}MgN_7Pt$ = 1260.5. Found = 1260.3 $(M)^+$.

[($C_7H_{15}O$-trpy-PO_3Et_2Pt(C≡CC_6H_4C≡C−MgP)]PF_6 (20). Yield 90%. R_f = 0.20 on neutral alumina eluted with CH_2Cl_2/CH_3OH (98:2). ^{1}H NMR (400 MHz, d_6-DMSO) δ: 10.26 (s, 1H), 9.77 (d, 2H, ^3J = 4.8 Hz), 9.40 (d, 2H, ^3J = 4.8 Hz), 9.07 (m, 2H), 8.89 (d, 2H, ^3J = 4.6 Hz), 8.83 (d, 2H, ^3J = 4.6 Hz), 8.62 (m, 2H), 8.46 (m, 2H), 8.21 (m, 2H), 8.09 (d, 2H, ^3J = 7.9 Hz), 8.05 (s, 4H), 7.87 (m, 2H), 7.85 (s, 2H), 7.70 (d, 2H, ^3J = 7.9 Hz), 4.23 (m, 2H), 1.54 (s, 36H), 0.8−1.55 (m, 13H). IR (KBr disk, ν/cm^{-1}): 2961 (m), 2867 (m), 2180 (s), 2110 (s), 1600 (s), 1210 (s), 1068 (m), 778 (s). MS−FAB (*m*/*z*) Calcd for $C_{80}H_{80}MgN_7OPt$ = 1375.6. Found = 1375.6 $(M)^+$.

Results

Preparations of the Compounds. The general synthetic route for the preparation of the new molecular systems is summarized in Scheme 2.

The synthesis of the dyads **15**−**20** required the initial preparation of the two key building blocks, namely, a metalloporphyrin (modules **10** and **11**) and a platinum chloro terpyridine complex (modules **4**−**6**). The porphyrin module **8** was easily available from a Sonogashira cross-coupling reaction using Lindsey conditions[23] between the corresponding 15-bromo-5,10-diaryl porphyrin[24] and 1-ethynyl-4-triisopropylacetylene-benzene **7**[25] followed by desilylation with fluoride anion. The terpyridine ligands **1** and **3** were prepared by modification of the literature procedures. The 4′-diethylphosphonate-2,2′:6′,2″-terpyridine **1** was previously described by Grätzel and co-workers[26] from a palladium

(23) Wagner, R. W.; Johnson, T. E.; Li, F.; Lindsey, J. S. *J. Org. Chem.* **1995**, *60*, 5266.
(24) (a) Uyeda, H. T.; Zhao, Y.; Wostyn, K.; Asselberghs, I.; Clays, K.; Persoons, A.; Therien, M. J. *J. Am. Chem. Soc.* **2002**, *124*, 13806. (b) Shediac, R.; Gray, M. H. B.; Uyeda, H. T.; Johnson, R. C.; Hupp, J. T.; Angiolillo, P. J.; Therien, M. J. *J. Am. Chem. Soc.* **2000**, *122*, 7017.
(25) Zehner, R. W.; Parsons, B. F.; Hsung, R. P.; Sita, L. R. *Langmuir* **1999**, *15*, 1121.
(26) Zakeeruddin, S. M.; Nazeeruddin, M. K.; Pechy, P.; Rotzinger, F. P.; Humphry-Baker, R.; Kalyanasundaram, K.; Grätzel, M.; Shklover, V.; Haibach, T. *Inorg. Chem.* **1997**, *36*, 5937.

Table 1. Electrochemical Data for Compounds **10**−**18**[a]

	porphyrin		Pt complex		
	reduction $E_{1/2}$ (V)	oxidation $E_{1/2}$ (V)	reduction $E_{1/2}$ (V)	oxidation $E_{1/2}$ (V)	ΔG_{CS} (eV) from porphyrin
10	−1.19	0.84			
11	−1.24	0.71			
12			−0.61	1.23	
13			−0.79	1.05	
14			−0.90	0.94	
15	−1.17	0.79	−0.59		−0.59
16	−1.20	0.83	−0.80		−0.34
17	−1.21	0.78	−0.94		−0.26
18	−1.14	0.70	−0.58		−0.66
19	−1.29	0.70	−0.79		−0.45
20	−1.28	0.70	−0.93		−0.31

[a] Recorded in dimethylformamide with 0.1 M Bu_4NPF_6 as the supporting electrolyte; scan rate: 100mV/s; all potentials referenced vs SCE. $E_{1/2} = (E_{pa} - E_{pc})/2$; E_{pa} and E_{pc} are peak anodic and peak cathodic potentials, respectively. ΔG_{CS} is calculated from Weller eq 1.

catalyzed cross-coupling reaction between the 4′-bromo terpyridine and diethyl phosphite. We showed that the replacement of the 4′-bromo terpyridine by 4′-triflate terpyridine was beneficial, because it avoids the preparation of 4′-bromo terpyridine that requires the costly lachrymator phosphorus oxybromide reagent and it afforded 4′-phosphonate terpyridine **1** with a much higher yield (92%). Terpyridine substituted by the ether substituent was obtained by the nucleophilic substitution of the corresponding pyridone with bromoheptane in an 80% yield. The chelation of terpyridines **1**−**3** with platinum involved heating the ligand with $Pt(COD)Cl_2$[20] (COD = cycloocta-1,5-diene) in water.[21] An anion methathesis reaction with a solution of sodium tetrafluoroborate led to colored precipitates **4**−**6** with high yields (>90%). The chloro platinum complexes **4**−**6** were subsequently reacted with alkyne **7**, **9**, or **11** in the presence of a catalytic amount of copper iodide and triethylamine and led to the formation of an acetylide platinum bond with good yields.[3,11]

Electrochemical Study. Cyclic voltammetry has been performed in DMF to determine the redox potentials of the dyads **15**−**20**. The electrochemical data are collected in Table 1. Half-wave potentials ($E_{1/2}$) were confirmed by square-wave voltammetry, and they are in excellent agreement with the values found by cyclic voltammetry.

The attributions of the redox processes have been made by comparison with the reference compounds and are in complete agreement with those reported by other groups for similar electroactive units.[4,10,27] For dyads **15**−**20**, in the anodic region, one reversible wave was observed at around 0.8 V, which can be confidently assigned to the oxidation of the porphyrin macrocycle because platinum oxidation potentials on reference complexes **12**−**14** are higher than 0.9 V and the oxidation potentials of the reference zinc and magnesium porphyrin **10** and **11** occur around 0.8 V.[28]

In the cathodic region, both the porphyrin and platinum complexes display several electrochemical processes. In the potential range −0.6 to −0.9 V, the first reversible one-electron reduction couple can be assigned to the platinum terpyridine complex. With reference to the other studies on platinum polypyridine complexes,[10,14,29] this reduction is most probably localized on the terpyridine ligand, but some contribution of the platinum metal may also exist. It is interesting to observe that the position of this redox couple is strongly affected by the substituent on the terpyridine. An electron withdrawing group, such as phosphonate, stabilizes the reduced terpyridine and makes the reduction more easily accessible at a lower potential, whereas an electron donating substituent, such as ether, increases the energy of the π^* LUMO orbital, thereby increasing the reduction potential of the complex. This expected trend is clearly observed in the reference platinum complexes **12**−**14** as well in the dyads **15**−**20**. The second reduction wave located in the range of −1.1 to −1.3 V is assigned to the porphyrin reduction because waves at comparable potentials were found in the reference porphyrins. These results, coupled with the luminescence study (see below), give the energetics for the photoinduced electron transfer processes from the porphyrin excited singlet state (cf. Table 1).

Electronic Absorption Spectra. The electronic absorption spectra of the molecules described in this study have been recorded in dimethyl formamide (DMF) where all of the compounds are soluble. The UV−vis absorption data are summarized in Table 2.

The absorption characteristics of the platinum(II) terpyridyl acetylide complexes **12**−**14** are in good agreement with those reported by other groups for similar structures (Figure 1a,b).[10,11] They display intense absorption bands in the UV region ($\epsilon \approx 5 \times 10^4\ M^{-1} \times cm^{-1}$) that are assigned to $\pi-\pi^*$ transitions localized on terpyridine (cf. Figure 1a). The lower-energy broad absorption band located around 420 nm is generally assigned to a MLCT transition.[10,11] The most recent molecular orbital calculations made on this type of complex have shown that the highest lying occupied orbitals (HOMOs) contain an important contribution of both platinum and an alkyne ligand.[29,31] Therefore, the broad absorption around 420 nm is probably not a pure MLCT transition but rather (what is designed as) a MMLL′CT transition (mixed-metal-ligand-to-ligand charge transfer) already described by Eisenberg for platinum diimine dithiolate complexes.[2] In this type of transition, the electron density originates from an orbital of a mixed metal and acetylide composition and shifts to an unoccupied π^* orbital localized on the terpyridine ligand. The position of this band is very sensitive to the substituent born on the terpyridine ligand. This is consistent with the well-known participation of the π^* LUMO of the terpyridine into the MMLL′CT electronic transition. An electron withdrawing substituent such as diethyl ester phosphonate (molecules **12**, **15**, and **18**) decreases the energy of

(27) Redmore, N. P.; Rubtsov, I. V.; Therien, M. J. *J. Am. Chem. Soc.* **2003**, *125*, 8769.
(28) O'Shea, D. F.; Miller, M. A.; Matsueda, H.; Lindsey, J. S. *Inorg. Chem.* **1996**, *35*, 7325.
(29) McInnes, E. J. L.; Farley, R. D.; Rowlands, C. C.; Welch, A. J.; Rovatti, L.; Yellowlees, L. J. *J. Chem. Soc., Dalton Trans.* **1999**, 4203.
(30) Calvert, J. M.; Caspar, J. V.; Binstead, R. A.; Westmoreland, T. D.; Meyer, T. J. *J. Am. Chem. Soc.* **1982**, *104*, 6620.
(31) (a) van Slageren, J.; Klein, A.; Zalis, S. *Coord. Chem. Rev.* **2002**, *230*, 193. (b) Fernandez, S.; Fornies, J.; Gil, B.; Gomez, J.; Lalinde, E. *J. Chem. Soc., Dalton Trans.* **2003**, 822.

Table 2. Absorption and Luminescence Data for Compounds **8**−**20**[a]

	absorption characteristics	luminescence			
	λ_{max} (ϵ) nm (dm^3 mol^{-1} cm^{-1})	λ_{em} (nm)	E_{0-0} (eV)	τ_{em} (ns)	Φ_{em}[b]
10	443 (257 000), 572 (8200), 623 (16 100)	630, 688	1.97	3.6	0.15
11	226 (17 200), 277 (17 700), 314 (18 100), 442 (290 000), 539 (3300), 578 (11 500), 629 (29 000)	640, 652	1.94	7.6	0.31
12	294 (53 500), 308 (44 400), 356 (11 500), 468 (6400)	∼670	∼2.1[c]	20	0.003
13	292 (54 000), 309 (42 200), 348 (14 600), 446 (8200)	∼640	∼2.2[c]	40	0.006
14	292 (45 100), 305 (38 000), 377 (12 700), 435 (6700)	605	∼2.3[c]	60	0.01
15	286 (55 300), 318 (36 400), 337 (27 400), 360 (26 500), 446 (222 900), 574 (13 700), 628 (30 900)	635, 690	1.97	<0.04[d]	0.012
16	445 (209 000), 574 (11 200), 626 (25 300)	632, 686	1.97	<0.04[d]	0.024
17	388 (25 300), 309 (19 100), 321 (13 000), 337 (17 900), 446 (135 000), 574 (7000), 626 (17 500)	634, 696	1.97	<0.04[d]	0.018
18	265 (44 000), 288 (43 000), 307 (33 600), 322 (33 300), 337 (31 100), 446 (300 000), 536 (7400), 580 (13 800), 633 (39 000)	652, 702	1.94	<0.04[d]	0.034
19	266 (32 300), 286 (32 700), 316 (24 700), 446 (219 000), 534 (4900), 580 (10 100), 632 (29 700)	652, 703	1.94	<0.04[d]	0.009
20	265 (67 100), 286 (43 100), 308 (33 400), 322 (33 200), 337 (31 000), 446 (356 300), 533 (6200), 580 (13 700), 632 (39 600)	651, 702	1.94	<0.04[d]	0.021

[a] Recorded in dimethylformamide at room temperature. [b] Measured with ZnTTP (Φ = 0.040)[4] or Ru(bpy)$_3$(PF$_6$)$_2$ (Φ = 0.062)[30] (for Pt emission) in CH_3CN as standards. [c] From emission maxima at 77 K. [d] Additional components corresponding to the unquenched porphyrin were attributed to impurities.

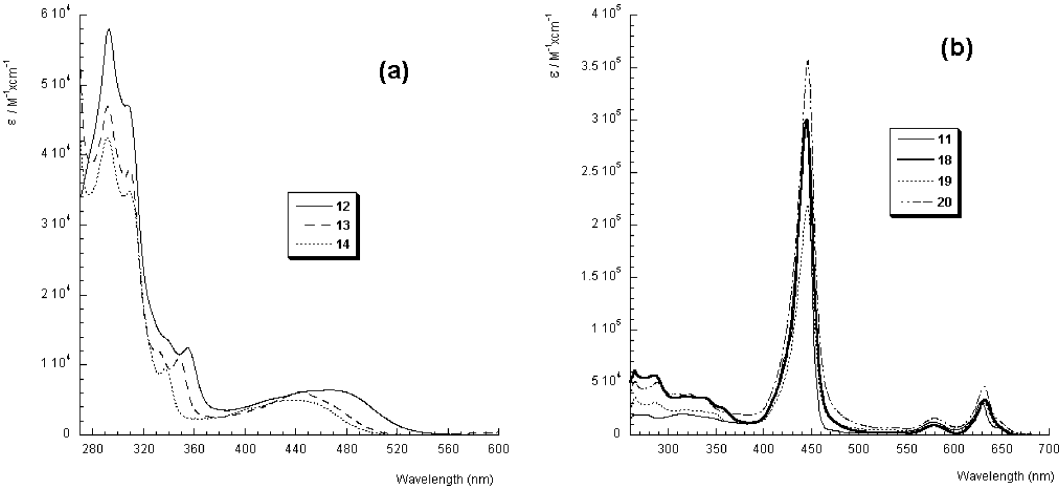

Figure 1. Electronic absorption spectra recorded at room temperature in DMF: (a) reference platinum(II) terpyridine arylacetylide complexes **12**−**14** and (b) the magnesium porphyrin dyads **18**−**20** along with the reference magnesium porphyrin **11**.

the LUMO pyridine orbital and, hence, leads to a lower energy MMLL′CT absorption. Conversely, an electron donating substituent such as ether (molecules **14**, **17**, and **20**) raises the π*(terpy) energy, thus increasing the energy of the MMLL′CT transition, which results in a blue shift of the absorption band (cf. Table 2). These substituent effects were apparent from the position of the emission wavelength maxima that reflect the energy level order of the lowest MMLL′CT excited state (see below). It is important to observe that the MMLL′CT transition of the platinum complexes has a low absorption coefficient ($\epsilon \approx 5 \times 10^3$ M^{-1} cm^{-1}) compared to that of the porphyrin transition in this region (cf. Table 2).

Porphyrin Modules. The porphyrin chromophores feature intense absorptions in the visible region. The introduction of a π-conjugated spacer that electronically interacts with the porphyrin units leads to a decrease of the energy of the porphyrin electronic transitions and an inversion of the relative Q-band intensities.[16] Changes in the relative transition strengths for Q(0,0) and Q(1,0) bands have been explained by Gouterman: Abs[Q(0,0)]/Abs[Q(1,0)] is proportional to the square of the energy difference $E(a_{2u} - e_g) - E(a_{1u} - e_g)$, where the latter corresponds to the energies of the singlet transitions.[32] Thus, smaller Q(1,0) bands indicate that the energy difference between singlet transitions is relatively large in these porphyrins, as compared to those of tet-

raarylporphyrins. This results from the attachment of a conjugated bridge at the 5 meso position, which electronically communicates with the porphyrin core, introducing an asymmetry that splits the degenerate *x*- and *y*-polarized transitions. Similar effects have been reported previously for *meso*-ethynyl-susbtituted porphyrins.[16,27] In addition, a broadening of the Soret band was seen, which was attributed to the splitting of the *x* and *y* components. In the UV region of the dyads **15**−**20**, both the porphyrin and Pt moieties show moderate to strong absorption.

Porphyrin−**Platinum Complex Dyads.** The absorption spectra of dyads **18**−**20** are shown in Figure 1b. The spectra of dyads **15**−**17** containing the zinc porphyrin are very similar in terms of shape and position of the absorption maxima (cf. Table 2). The visible part of the spectrum is dominated by the intense absorption bands of the porphyrin unit that give rise to intense Soret bands associated with transitions to the second excited singlet state.[4] The two Q bands around 630 and 580 nm are ascribed to 0,0 and the first vibronic transition to the first excited singlet state, respectively.[4] In the dyads, the Soret transition of the porphyrin, located around 420 nm, overlaps with the MMLL′CT transition of the platinum complex. The MMLL′CT transition is, therefore, not discernible because of its much lower molar absorptivity. As a result, selective excitation of the platinum complex is impossible, whereas that of the porphyrin unit is easily feasible by light irradiation in the Q bands of the porphyrin. Absorption of the platinum complex in the UV region is more intense than that of the porphyrin unit; thus, the $\pi-\pi^*$ transition of the terpyridine fragment can be clearly distinguished (around 290, 320, and 340 nm), although they overlap with the porphyrin transitions. It can be concluded that in dyads **15**−**20,** the absorption spectra are almost a superposition of the spectra for the individual chromophores, but with some significant differences. The porphyrin absorption bands are slightly red-shifted (3−5 nm), and the Soret band is broader and has a less intense maximum than the corresponding reference porphyrins **10** or **11** (cf. Figure 1b), although the latter already contain the arylacetylide bridge. Moreover, the intensity of the Q(1,0) absorption band is lower relative to that of Q(0,0) band than it is in the references. These changes indicate a significant electronic interaction between the porphyrin and the platinum complex that further splits the energies of the *x*- and *y*-polarized transitions.

Also, the electrochemical results suggest a weak but noticeable interaction between the terpyridine and porphyrin units, seen as a less negative potential for porphyrin reduction when the terpyridine has an electron withdrawing phosphonato substituent (**15** and **18**). It is interesting that the effect of the substituent in **15** and **18** is mediated over such a long distance, over the platinum metal ion and the *para*-diethynyl−phenyl bridge. Similar results were reported in ref 27 where a significant interaction over ethylnyl−phenyl spacers in porphyrin−diimide dyads has been observed as a change in the porphyrin redox potentials depending on the identity of the diimide.

(32) Spellane, P. J.; Gouterman, M.; Antipas, A.; Kim, S.; Liu, Y. C. *Inorg. Chem.* **1980**, *19*, 386.

Steady-State Luminescence Spectra. The luminescence spectra were recorded in a deaerated DMF solution for all molecules. The emission data are listed in Table 2. The porphyrins display emission spectra that are typical for this class of fluorescent dyes.[4,27] The energy of the lowest porphyrin singlet excited state (E_{0-0}) was calculated from the average of the 0−0 Q-band maximum in the room-temperature absorption and fluorescence spectra. For the triplet MMLL′CT state of the platinum complex, E_{0-0} was estimated from the first emission band maximum in a solvent glass at 77 K where spectral distortion is minimized. Still, the degree of spectral distortion that suggests the emission maximum somewhat underestimates E_{0-0}.

The platinum complex emission is attributed to phosphorescence from the MMLL′CT excited state, and the spectra are very similar to those reported for related platinum terpyridyl arylacetylide complexes.[10] The emission maxima show that the energy of the MMLL′CT excited state decreases steadily across the series of complexes **14** > **13** > **12** as the electron withdrawing strength of the substituents increases. This is consistent with the MMLL′CT nature of the emissive state, which involves the terpyridine π^* LUMO orbital of the complex. The room-temperature emission lifetime was 60, 40, and 20 ns for **14**, **13**, and **12**, respectively. The emission quantum yield was ca. 1×10^{-2} for **14** and decreased in parallel to the lifetime in the order **14** > **13** > **12**.

Fluorescence spectra of the reference porphyrins ZnP **10** and MgP **11** exhibit the typical Q(0,0) and Q(0,1) emission bands around 630 and 690 nm, respectively.[4] The fluorescence emission spectra clearly show that ZnP and MgP have very similar emission energies (around 1.9 eV), although the ZnP excited state is slightly higher than that of MgP, which is consistent with what is generally observed for tetraarylporphyrins.[4]

The luminescence spectra of both ZnP and MgP, containing dyads **15**−**20**, were measured by excitation at the maximum of the first Q band of the porphyrin where the photons are exclusively absorbed by the porphyrin unit. The fluorescence intensity of the porphyrin in dyads **15**−**20** is almost quantitatively quenched by the nearby platinum complex compared to the reference porphyrin **10** or **11** (cf. Table 2).

The time-resolved fluorescence after excitation with 150 fs laser pulses at 400 nm showed a single-exponential decay for the reference porphyrins **10** and **11** with lifetimes of 3.6 and 7.6 ns, respectively. The dyads instead showed a very rapid decay component (τ < 40 ps) followed by a slower component with a lifetime of a few nanoseconds, very similar to that for the corresponding reference porphyrin. This suggests that the porphyrin singlet excited state (S_1) in the dyads is quenched on a time scale shorter than what could be resolved in these experiments (τ < 40 ps). This was supported by the femtosecond transient absorption experiments described below. The unquenched emission decay component must correspond to some porphyrin impurity that is not attached to an active Pt quencher. Because the short lifetime component could not be resolved, the relative

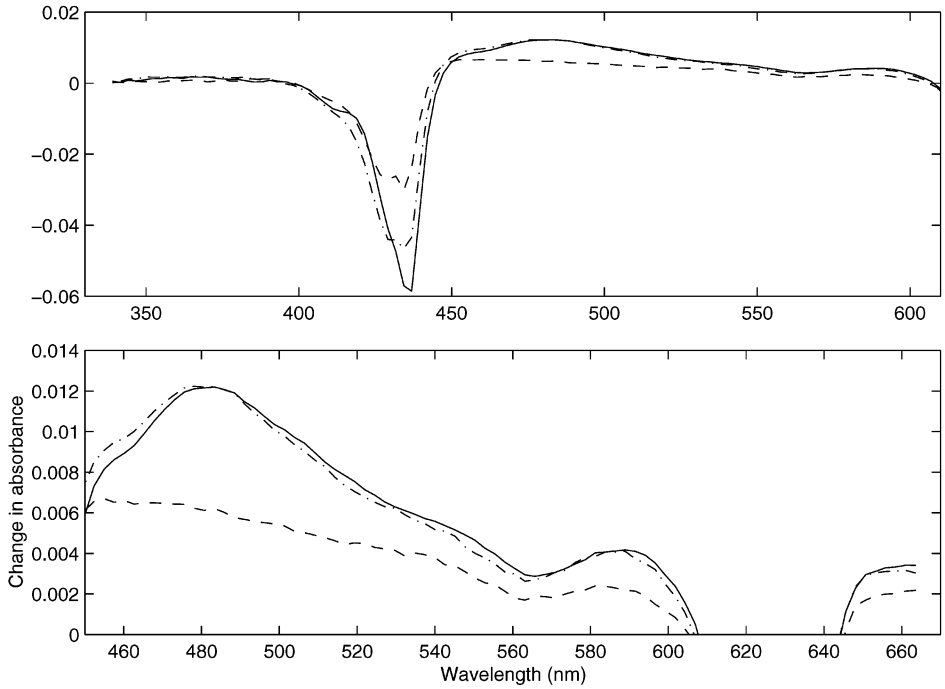

Figure 2. Transient absorption spectra of **10** after excitation with a 150 ps laser pulse at 630 nm. The spectra shown are at 1 ps (solid), 100 ps (dot−dashed), and 4 ns (dashed) after excitation.

amplitude of the unquenched component could not be determined in these experiments. The fluorescence yields and the transient absorption results given below suggest that this component corresponds to ca. 10% of the dyad samples and, hence, that it dominates the fluorescence spectra.

Transient Absorption. The reference porphyrins **10** and **11** as well as the dyads were studied by transient absorption spectroscopy following excitation with 150 fs laser pulses at 630 nm. Immediately after the pulse, the transient spectra of **10** and **11** are typical for the lowest excited state (S_1) of similar porphyrins, for example, ZnTPP,[4] with a maximum signal at 470 nm (cf. Figure 2). Some spectral dynamics are seen on the time scale of ca. 10 ps (not shown), particularly on the red side of the Soret band (430−450 nm). This is indicative of some relaxation in the S_1 state, possibly due to rotation of the phenyl group of the bridge.[27] On the much longer time scale of some nanoseconds, this develops into a spectrum that can be attributed to the lowest excited triplet state (T_1), with a transient absorption maximum at ca. 460 nm. The signal decay at 470 nm, where no picosecond dynamics are seen, was used to follow the development from the S_1 to the T_1 spectrum. The decay can be fitted to a single exponential with a lifetime of ca. 2.5 ns that, given the limited length of the optical delay line, is in good agreement with the S_1 lifetime determined from the fluorescence decay above. It is clear from the recovery of both the Soret- and Q-band bleach that the S_1 state, to a large extent, decays to the ground state, suggesting a triplet yield of approximately 0.5, which is somewhat lower than, for example, ZnTPP.[4]

In all of the dyads **15**−**20**, the initial spectrum after the excitation pulse (cf. Figure 3) was in good agreement with the S_1 spectrum of the corresponding reference porphyrin. The lifetime of the S_1 state, however, was strongly reduced. Single-exponential fits to the transient absorption decay at 400−600 nm gave a S_1 lifetime of 2−20 ps for the different dyads (Table 3), leaving a small and long-lived ($\tau > 10$ ns) residual absorption with a spectral shape suggesting a T_1 state. The magnitude of this residual T_1 absorption relative to the reference **10** or **11** agreed with the relative fluorescence yield, suggesting that it arose from a fraction of unquenched porphyrins rather than from a reaction in the intact dyads. No other species could be resolved in the transient spectra. Importantly, the recovery of the Soret- and Q-band bleach followed the same kinetics as the S_1 transient absorption decay, both in terms of time constant and relative amplitude, showing that the ground state was repopulated with the same kinetics as the S_1 decay.

Discussion

In this paper, we will focus the discussion only on the potential deactivation processes from the porphyrin excited singlet state because selective light excitation of the platinum fragment is impossible, and both the emission and transient absorption changes of the platinum unit are very weak compared to those for the porphyrin.

In all dyads **15**−**20**, the porphyrin fluorescence is quenched compared to that of the reference porphyrin (**10** or **11**). The transient absorption shows that the lifetime of the first porphyrin singlet excited state (S_1) is much shorter in the dyads ($\tau = 2-20$ ps) than in the model porphyrins **10** ($\tau =$ 3.6 ns) and **11** ($\tau = 7.6$ ns). This shows that the covalent attachment of a platinum complex to the porphyrin imparts additional deactivation pathways compared to the model porphyrin.

One major deactivation pathway in the reference porphyrins is intersystem crossing to the triplet (T_1) state. An

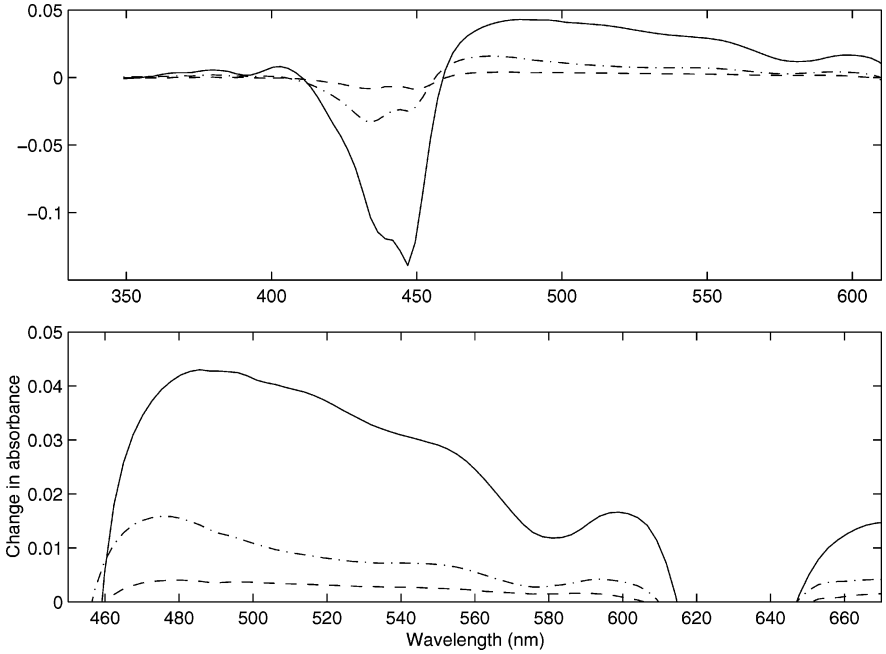

Figure 3. Transient absorption spectra of dyad **16** after excitation with a 150 ps laser pulse at 630 nm. The spectra shown are at 1 ps (solid), 10 ps (dot−dashed), and 4 ns (dashed) after excitation.

Table 3. Quenching Time Constants for the Porphyrin S_1 State in Dyads **15**−**20** Attributed to an Electron Transfer (See Text)

dyad	τ_q (ps)	dyad	τ_q (ps)
15	2	**18**	2
16	6	**19**	5
17	20	**20**	10

enhancement of this process has been reported in Zn(II) porphyrin-acceptor dyads with paramagnetic metals in the acceptor moiety,[33] presumably because of spin−spin coupling. An enhanced intersystem crossing could occur also with heavy metals such as platinum, as the result of an increased spin−orbit coupling. This should lead to the efficient formation of the triplet state, however. Instead, we see a regeneration of the ground state with the same kinetics as the S_1 decay. Thus, an enhanced intersystem crossing cannot be a significant contribution to the rapid S_1 deactivation in the dyads (the very low yield of triplet observed corresponds very well to the fraction of unquenched porphyrin and is, thus, not the result of reactions in the reactive dyads).

It has recently been shown by Yam and co-workers that platinum terpyridine acetylide complexes can form aggregates both in the solid state and in solution.[34] Porphyrins, which are hydrophobic π-aromatic systems, are also prone to aggregation in polar solvents. Therefore, it can be anticipated that dyads **15**−**20** could form aggregates in solution. These aggregates could also be responsible for fluorescence quenching by a self-quenching process that has been encountered many times with aggregated dyes. The ground state and transient absorption spectra of the dyads show no sign of aggregation, however, and all of the quenching kinetics were single exponential. Moreover, the degree of quenching (ca. 90% of the amplitude) was the same in the fluorescence yield and the transient absorption experiments, despite the large difference in concentration, <0.01 mM versus 0.2 mM. We, thus, believe that the fraction of aggregates is small and that it is not an important contribution to the observed quenching.

Other potential deactivation processes of the porphyrin singlet excited state are the photoinduced energy or electron transfer. The energy transfer from the excited singlet state of the porphyrin to the platinum complex can be ruled out on the basis of the free energy of this process, as determined from the absorption and emission spectra of the components. Singlet-to-singlet energy transfer is extremely unlikely because the ^{1}MMLL′CT state lies far above the S_1 state of the porphyrin (1.9 eV). The energy of the lowest singlet excited state (^{1}MMLL′CT) of the platinum complex can be estimated from the red edge of the absorption band of the reference complexes **12**−**14**. This is found to be in the range of 510−470 nm, corresponding to an excited-state energy of 2.4−2.6 eV (cf. Table 2). A rapid (2−20 ps) S_1-to-^{3}MMLL′CT energy transfer from the porphyrin is also unlikely because the latter state is at 2.1−2.3 eV (cf. Table 2) in the series of dyads, that is, at 0.2−0.4 eV above the porphyrin S_1 state. Furthermore, no products of an energy transfer process are seen, so that, if it occurred, the decay of the platinum MMLL′CT state must be much faster than the rate of its formation, that is, much faster than 2 ps for **15** and **18**. Finally, an energy transfer to the singlet states of the bridge can be excluded, because the lowest singlet excited states of related phenylethynyl compounds are located at an energy of >3 eV.[35,36]

(33) (a) Asano-Someda, M.; Kaizu, Y. *Inorg. Chem.* **1999**, *38*, 2303. (b) Pettersson, K.; Kils, K.; Mrtensson, J.; Albinsson, B. *J. Am. Chem. Soc.* **2004**, *126*, 6710.

(34) Yam, V. W.-W.; Wong, K. M.-C.; Zhu, N. *J. Am. Chem. Soc.* **2002**, *124*, 6506.

(35) Biswas, M.; Nguyen, P.; Marder, T. B.; Khundkar, L. R. *J. Phys. Chem. A* **1997**, *101*, 1689.

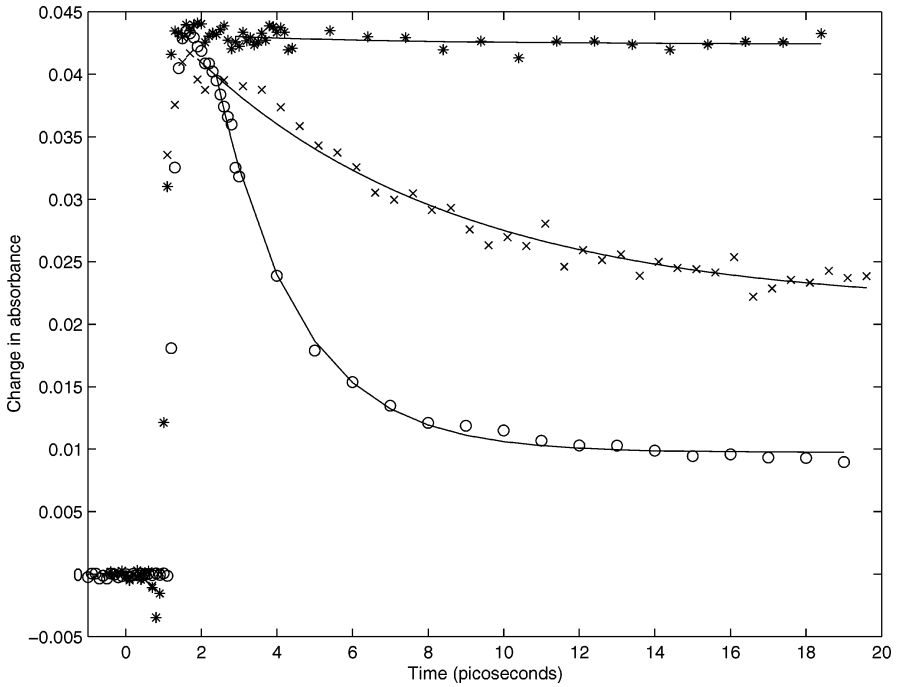

Figure 4. Transient absorption traces at 500 nm for **10** (stars), **15** (circles), and **16** (crosses) in the same experiments as those shown in Figures 2−3. The lines are single- (**10**) or double-exponential (**15** and **16**) fits to the data (see text).

The reaction free energies for the photoinduced electron transfers are gathered in Table 1. The photoinduced electron transfer process is clearly exergonic, and it can be anticipated that this process gives an important contribution in the excited-state deactivation of the porphyrin. The calculations of the photoinduced electron transfer driving force are based on the Rehm−Weller equation[37] (eq 1), where E_{0-0}(P) is the zero−zero excitation energy of the porphyrin and $E^0_{Ox}(P^+/P)$ and $E^0_{Red}(Pt^+/Pt^0)$ are the reduction potentials for the porphyrin donor and the platinum complex acceptor couples, respectively.

$$\Delta G^\circ = E^0_{Red}(Pt^+/Pt^0) - E^0_{Ox}(P^+/P) - E_{0-0}(P) \qquad (1)$$

The potentials were determined in the same solvent (DMF) as that used for the photochemical experiments. Also, the Coulombic work term is omitted because the electron transfer leads only to a charge shift, with one net neutral species in both the reactant and the product states. The exergonicity of the electron transfer process varies in a large range in the series of dyads, from fairly favorable in dyad **17** ($\Delta G^\circ = -0.26$ eV) to very favorable in dyad **18** ($\Delta G^\circ = -0.66$ eV). The relative rate constant of the S_1 decay in the series of dyads varies with the driving force for an electron transfer, in agreement with the Marcus expression[36] (cf. Figure 4)

$$k_{ET} = A \exp\left[-\frac{(\Delta G^0 + \lambda)^2}{4\lambda RT}\right] \qquad (2)$$

where ΔG^0 is the driving force according to eq 1 and λ is the reorganization energy. In Figure 5, the parabolic curve is a fit to the data according to eq 2, with the preexponential factor (A) as the only floating parameter and λ set to 0.65 eV, which is a reasonable guess for this type of system.[38] With few data points, which span only a part of the putative Marcus curve, the result cannot, on its own, be taken as evidence for an electron transfer, but it shows clearly that the results are in agreement with a rapid electron transfer from the excited porphyrin unit. The lack of a detectable charge transfer intermediate implies that the subsequent recombination is faster than the initial electron transfer. This was previously observed for Zn(II) porphyrin−diimide dyads linked via the same type of bridging molecules,[27] and the time scale of the initial electron transfer was very similar to that of the present case.

An electron transfer via arylethynyl bridging units has been discussed in terms of a significant delocalization of the donor or acceptor state over the bridge.[27,35] This effect may be entirely different for the charge separation and the subsequent recombination reaction, so that the bridge may favor one of the reactions over the other. For a series of phenylethylnyl-bridged zinc(II) porphyrin−diimide dyads, Therien and co-workers[27] suggested that the porphyrin cation of the charge separated state was delocalized over the bridge, whereas the S_1 excited state was not, on the basis of fits of the solvent dependence of the rate constants. When the bridge of one of the dyads was elongated with another phenylethynyl unit, however, the rate of charge separation was only 3 times slower, whereas the subsequent recombination was reduced as much as 500 times. The much weaker distance dependence for charge separation in that case suggests that this type of bridge instead selectively mediates charge separations over long distances. Possibly, this occurs by delocalization of the

(36) (a) Hirata, Y.; Okada, T.; Mataga, N.; Nomoto, T. *J. Phys. Chem.* **1992**, *96*, 6559. (b) Hirata, Y.; Okada, T.; Nomoto, T. *J. Phys. Chem.* **1993**, *97*, 9677.

(37) Rehm, D.; Weller, A. *Isr. J. Chem.* **1970**, *8*, 259.

(38) Marcus, R. A.; Sutin, N. *Biochim. Biophys. Acta* **1985**, *811*, 265.

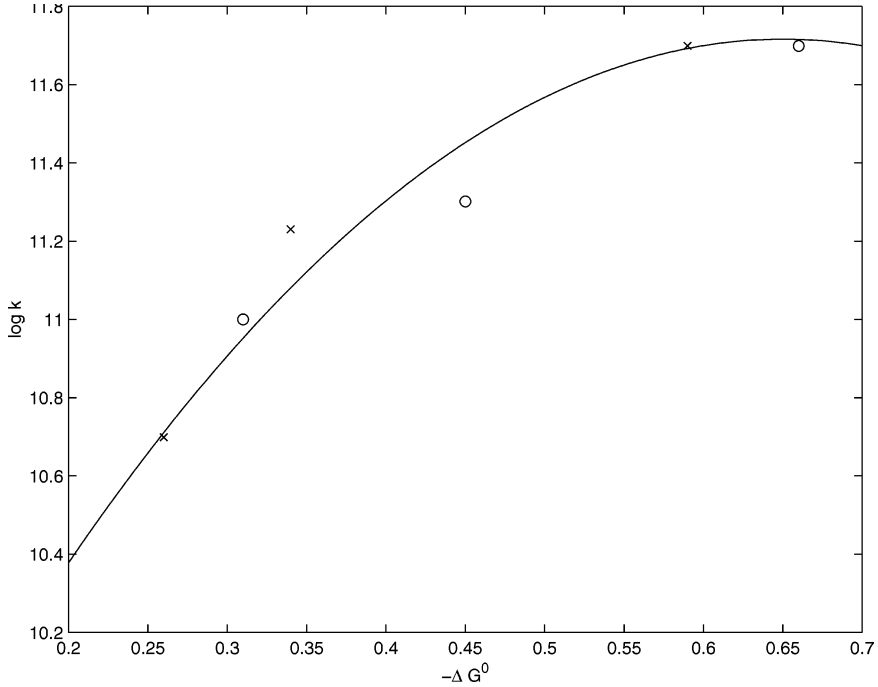

Figure 5. Quenching rate constant as a function of electron transfer driving force for dyads **15**−**20**. The line is a fit to the Marcus free energy dependence of the electron transfer rate constant (eq 2).

porphyrin excited state over the bridge, which is enhanced as the length of the π-conjugated bridge increases. It is, thus, of interest to examine the effect of an elongation of the bridge in the present porphyrin−Pt systems on the charge separation and recombination rates, to elucidate whether one reaction shows a weaker distance dependence than the other and whether this effect can be used to selectively favor charge separation.

In conclusion, an electron transfer from the porphyrin to the platinum unit seems to be the only reasonable explanation for the very rapid deactivation ($\tau = 2-20$ ps) of the lowest excited singlet state of the porphyrin in the dyads **15**−**20**. The deactivation rate constant shows a Marcus-type variation with a driving force for an electron transfer. The subsequent recombination of the charge transfer state is even more rapid, so that the regeneration of the ground state reactants follows the same kinetics as the decay of the porphyrin excited state. The results underscore the potential of phenyl−ethenyl bridges to promote very rapid electron transfers over long distances. The development of new systems with longer bridges, such as oligophenyl acetylene modules, is under way in our laboratory in order to try to slow the rate of the recombination process, while hopefully maintaining a rapid charge separation.

Acknowledgment. L.H. acknowledges financial support from the Knut and Alice Wallenberg Foundation and the Swedish Foundation for Strategic Research and a Research Fellow position from the Royal Swedish Academy of Sciences. Financial support by La Rioja University (Spain) for the salary of J.G. is gratefully acknowledged. This study was partially subsidized by the French Ministry of Research by the ACI "jeunes chercheurs" 4057.

Supporting Information Available: Phosphorescence emission spectra of the reference complexes **12**−**14** recorded at 77 K. This material is available free of charge via the Internet at http://pubs.acs.org.

IC048573Q